JOURNAL OF ENGINEERING SCIENCES

Volume 9, Issue 2 (2022)

Sapozhnykov Y., Zahorulko A., Peczkis G. (2022). Numerical simulation of 2-way FSI problem of face packing seal: Impact of parameters change. Journal of Engineering Sciences, Vol. 9(2), pp. E12-E27, doi: 10.21272/jes.2022.9(2).e3

Numerical Simulation of 2-Way FSI Problem of Face Packing Seal: Impact of Parameters Change

Sapozhnykov Y.[1*[0000-0002-9911-407X]], Zahorulko A.[1[0000-0002-6198-4643]], Peczkis G.[2[0000-0003-1820-3773]]

[1] Sumy State University, 2 Rymskogo-Korsakova St., 40007 Sumy, Ukraine;
[2] Silesian University of Technology, 2A, Academicka St., 44-100 Gliwice, Poland

Article info:
Submitted: September 15, 2022
Accepted for publication: December 8, 2022
Available online: December 12, 2022

***Corresponding email:**
y.sapozhnykov@cm.sumdu.edu.ua

Abstract. The article is devoted to creating a refined computer model of the face packing seal (FPS) based on the solution of the two-way fluid-structure interaction (2-way FSI) problem. An approach to the average gap was proposed based on the micro-space's working medium leakage between the friction pair's roughness elements. Three FPS designs were studied, in which the following operating parameters were alternately changed: inlet pressure, load factor, stuffing box parameters, and friction coefficient. Young's modulus, Poisson's ratio, and the thickness of the annular plate at the bottom of the stuffing box were also changed. The model was created considering the actual geometry of the FPS. The shaft rotation was considered by applying the rotation condition on the wall of the fluid model. The calculation was carried out using the ANSYS Multiphysics software. The results of the calculations were presented in the form of graphic dependences with a comparison of the hydrostatic and contact pressure distributions over the friction pair width. The values of the magnitudes of leakage from the changing parameters were presented. Based on the obtained results, an optimal combination of parameters was evaluated for the most efficient design of the FPS.

Keywords: stuffing-box, ANSYS Multiphysics, hydrostatic pressure, contact pressure, process innovation.

1 Introduction

For modern mechanical engineering, one of the essential criteria, in addition to energy efficiency, in compliance with accepted environmental standards [1, 2]. For pump units, this criterion is related to the leakage of the working medium into the environment. That is why one of the essential tasks today is the improvement of the existing systems of pump seals.

In addition, the need for pumping both liquid and gaseous substances is constantly increasing [3]. The most common type of seal is stuffing box seals, which are used both for sealing shafts of centrifugal pumps and for armature spindles.

Stuffing box seals have become widely used in pumping units that pump neutral media at normal temperatures. Until now, the stuffing-box remains the cheapest and easiest-to-use sealing material. For a long time, the designs of stuffing-box seals and the conformity of the packing to new operating conditions for various types of industries have been improved. Mainly, the seal's service life was increased while maintaining a low leakage rate.

The stuffing box has many options, as it is a central wire with braided fibers. Packings with fluoroplastic fibers (PTFE) have become widespread, as this material is often used as a sealant in fixed joints. In addition, the stuffing can be impregnated with liquid materials based on silicone, which ensures a low friction coefficient and, as a result, a low friction temperature.

Today, end mechanical seals are most often used to seal the shafts of centrifugal machines. Therefore, the most energy-efficient packing seal is the face packing seal of various modifications. Because of this, the improvement of this type of stuffing box seal is considered the most expedient [4]. This work will consider some structural improvements of the FPS.

In today's world, the process of improving any element or system is impossible without the use of computational technology. The existing software complexes are capable of processing huge arrays of data. They allow you to create any computer model with conditions as close as possible to real ones. Some problems, such as problems of hydroaeroelasticity, thermoelasticity, and other interdisciplinary issues, are quite complex to solve

analytically, and it is necessary to resort to numerical modeling of specific processes.

Now there are commercially available software packages ANSYS Multiphysics, STAR-CCM+, Open FOAM, etc., making it possible to create interdisciplinary models.

The fluid-structure interaction problem is the interaction of some solid moving body that deforms with an internal or surrounding fluid flow. This interaction can be stationary or oscillating. In oscillatory interactions, the stress induced in the rigid structure causes the body to move so that the source of deformation is reduced, and the solid body returns to its original state only to repeat the process.

In general, three types of problems of Fluid-structure interaction are considered:

1) the problem for a rigid body (Rigid Body FSI) is a problem of flow around a rigid body. In this case, there are no deformations of the solid body, and only the movement of the body in liquid or gas is considered;

2) the one-way fluid-structure interaction (1-way FSI) involves considering very small deformations of an elastic body under the action of hydrodynamic forces. This algorithm allows you to transfer data from the CFD solver to the Mechanical solver and vice versa;

3) the two-way fluid-structure interaction (2-way FSI) is solved when data is transferred in both directions between the fluid and solid models. This type of coupling is necessary for models with large deformations, such as a heart valve or thermal expansion problems, because the results of one model significantly change the boundary conditions and the result of another [5].

This work aims to create a computer model of the FPS, which is as close as possible to the real sample in terms of leakage indicators and the distribution of hydrostatic pressure in the friction pair. Determining the distribution of contact pressure in the friction pair is also necessary.

2 Literature Review

Until now, any calculations related to compatible problems were performed exclusively analytically based on the results of experiments [6, 7]. The obtained analytical dependences give an idea of the sealing process in the stuffing box seal. However, there was a problem in comparing the distribution of contact pressure in a friction pair, as it was impossible to determine it experimentally.

Later, with the help of the ANSYS software complex, it was possible to create simple models of FPS. The one-way FSI problem is solved in [8]. These models served as the foundation for creating and improving further models of gland seals.

Separately, it is essential to note that in works [9-12], the stuffing box is considered as a porous body with experimentally determined coefficients of porosity and permeability. At the same time, the FSI problem is not solved, and calculations are based on Darcy's law.

3 Research Methodology

The computer model of the FPS represents a sector of 1/6 of the sealing part (Figures 1, 2). Such a simplified model makes it possible to use less machine time for calculation. The model was developed with the help of the ANSYS software complex. This software complex allows you to solve various interdisciplinary problems, including the FSI problem. In this case, the two-way FSI problem is considered. The solution to this problem is based on a distributed approach with a strong coupling between the elements of the solver.

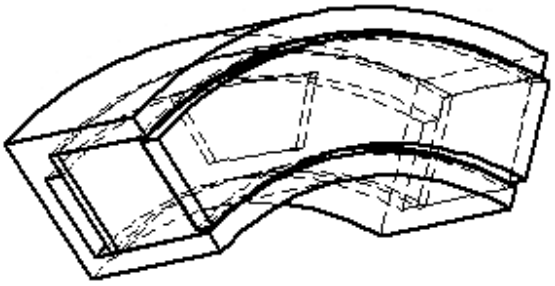

Figure 1 – General view of the FPS model

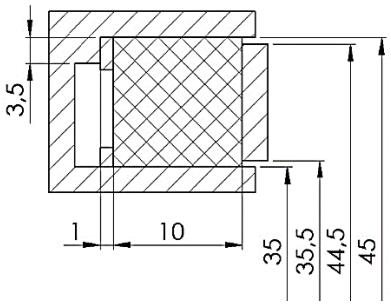

Figure 2 – Section of the FPS model and geometric dimensions

As a solid domain act (Fig. 3), packing chamber 1, packing ring 2, and bushing support disk 3. In the modernized version, the FPS has an annular plate (solid 4 and with grooves in the form of a trapezoid 5). Figure 4 shows two conditional lines, along which the hydrostatic and contact pressure distributions will be determined. The first line passes through the groove and divides the plate segment into two symmetrical parts. Conventional name - groove line. The second line runs along the edge of the plate segment and has the conventional nameplate line. The position of these two lines is chosen so that it is possible to see the difference in pressure distributions for the traditional design (Fig. 3 a) and for designs with an annular plate (Fig. 3 b, c).

The boundary conditions for the solid domain are as follows (Table 1, Figures. 3–5).

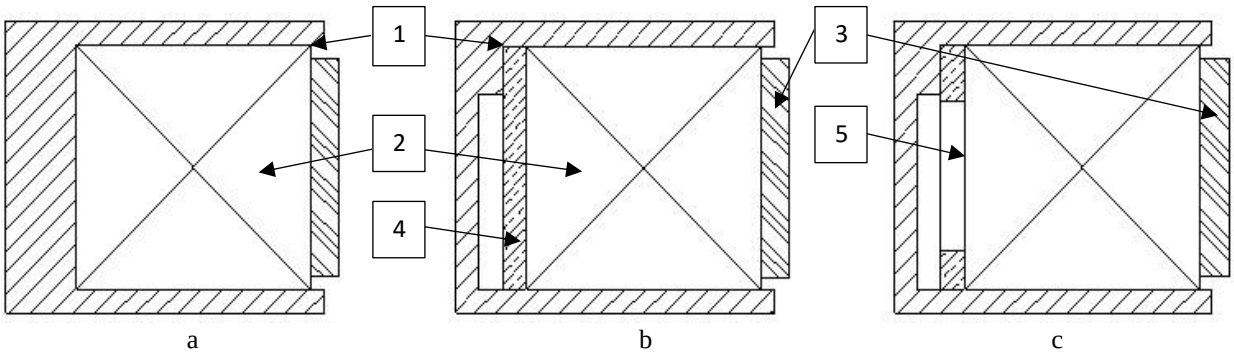

Figure 3 – FPS designs: a – traditional; b – with an annular plate at the bottom of the stuffing box; c – with grooves in the annular plate

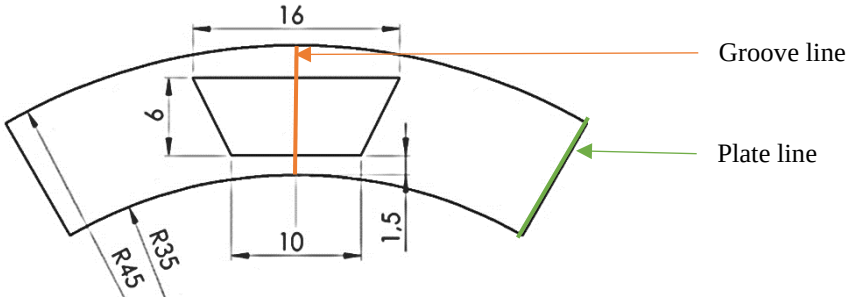

Figure 4 – Sketch and geometric dimensions of the groove in the plate

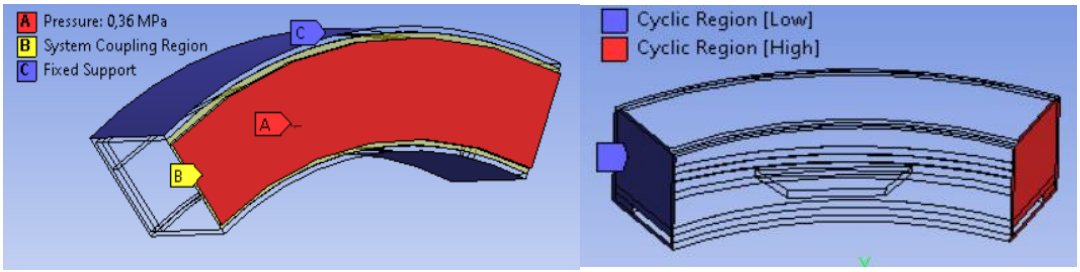

Figure 5 – Boundary conditions of the solid domain

Table 1 – Boundary conditions for the solid domain

No.	Structural element	Boundary condition
1	The walls of the packing chamber 1 (C on Fig. 5)	Fixed support
2	The surface between the annular plate 4/5 and the packing chamber 1	Frictional contact
3	The surface between packing ring 2 and packing chamber 1	Frictional contact
4	The surface between packing ring 2 and annular plate 4/5	Frictional contact
5	The surface between packing ring 2 and bushing support disk 3	Frictional contact
6	The surface of the stuffing box B on Fig.5	System coupling region
7	The surface of sleeve A on Fig.5	Pressure
8	Side surfaces of the model (Low, High in Fig.5)	Cyclic region

The fluid body model is based on the idea that the working medium flows in a friction pair along channels formed by micro-irregularities. In the sealing process, these micro-irregularities acquire an arbitrary shape and size within the main dimensions of roughness (protrusions and depressions) [13]. Thus, it can be concluded that leakage occurs through an averaged gap with a fixed size. Based on such a representation, it is possible to create a fluid domain that will interact with the stuffing box model. A finite-element mesh was created for such a fluid domain, and boundary conditions were determined (Table 2, Fig. 6).

The size of the averaged gap was chosen so that in the created model, the leakage rate coincided with the leakage determined in the experiment [14]. In the experiment, the traditional design of the FPS was studied, the shaft size was 40 mm, and the outer and inner radius of the stuffing box was 45 mm and 35 mm, respectively. Physical and mechanical parameters of the stuffing box: Young's

modulus – 50 MPa, Poisson's ratio – 0.4. For the seal operation mode: inlet pressure – 0.4 MPa, shaft rotation speed – 3000 rpm, the leakage rate is 1.1 l/h. This level of leakage in the computer model is satisfied with an average gap height of about 3 μm.

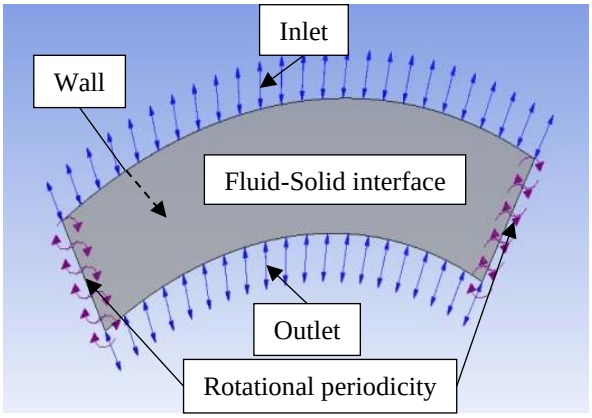

Figure 6 – Boundary conditions for the liquid domain

Table 2 – Boundary conditions of the fluid domain

No.	Surface name	Boundary condition
1	Inlet	Inlet
2	Outlet	Outlet
3	Wall	Wall
4	Fluid-Solid interface	System coupling
5	Symmetry	Rotational periodicity

When creating an FSI model, the first task is to connect two independent mesh domains together while considering the fundamental differences in the mesh formation of each domain. A Lagrangian mesh is used for FEA modeling, where the finite element mesh is fixed to the mass and moves in space as a function of the movement of the mass. In contrast, CFD modeling uses an Eulerian mesh, where a finite element is fixed in time and space with mass passing through the mesh [15].

FSI modeling has three main methods of data transfer between the fluid and solid domains: the Lattice-Boltzmann method, the fictitious domain, and the Arbitrary Lagrange-Euler method. In this work, the arbitrary Lagrange-Euler method is used, in which data transmission is carried out through a seamless interface (Fig. 7).

Processing of finite-element meshes introduces another classification of the analysis of the FSI problem. The two different classifications are conformal and non-conformal meshing methods. For the selected method of data transfer, it is not essential which method of grid creation will be chosen. It does not affect the result of calculations.

In this problem, a non-conformal type of connection between mesh elements of solid and liquid domains is used (Fig. 8)

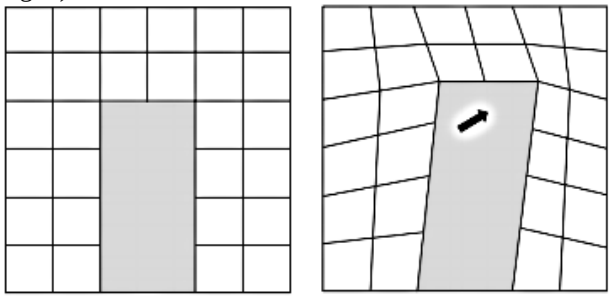

a b

Figure 7 – The black lines represent the fluid domain (Eulerian) mesh, and the gray body represents the solid (Lagrangian) mesh

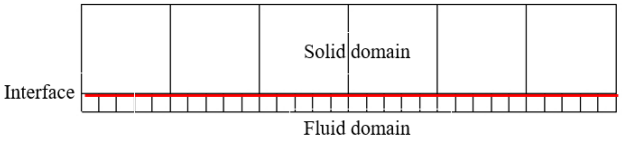

Figure 8 – Non-conformal connection between solid and liquid domain elements

The grid movement created by the arbitrary Lagrange-Euler method is shown from Fig. 7a to Fig. 7b.

The basic model of FPS was studied under the following conditions (Table 3).

Table 3 – Operating parameters and geometric dimensions

	Parameter	Marking	Size
1	Inlet pressure	P	0.4 MPa
2	Shaft rotation frequency	n	3000 rpm
3	The thickness of the annular plate	h	1 mm
4	The thickness of the averaged gap	h_{gap}	3 μm
5	The load factor of the support disk sleeve	K	1

The stuffing box has the following characteristics (Table 4):

Table 4 – Characteristics of the stuffing box

No.	Characteristic	Marking	Size
1	Size (in cross-section)	b	10x10 mm
2	Young`s modulus	E	50 MPa
3	Poisson's ratio	μ	0.4
4	Coefficient of friction	f	0.04

FPS designs with different parameter values were considered. The parameters were alternately changed in the following ranges (tab. 5)

Table 5 – Parameter change ranges

No.	Parameter	Marking	Magnitudes				
1	Load factor of the bushing support disk	*K*	0.85	0.90	0.95	1	1.1
2	Young`s modulus (MPa)	*E*	50	150	250	350	–
3	Poisson's ratio	*μ*	0.40	0.43	0.45	0.47	–
4	Inlet pressure (MPa)	*P*	0.40	0.80	1.20	1.60	–
5	Friction coefficient	*f*	0.04	0.06	0.08	0.10	–
6	Annular plate thickness (mm)	*h*	0.30	0.50	0.80	1	–

4 Results and Discussion

4.1 Parameter *K* influence analysis

As a result, to display the complete picture, a comparison of the graphs of the hydrostatic and contact pressure distribution along the friction pair width is presented (Figures 7–9). Such a comparison makes it possible to conclude the change in the direct contact zone of the stuffing box along the friction pair width.

First, it should be noted that the change in friction coefficients and Poisson's ratios have little effect on the distribution of hydrostatic and contact pressures.

Therefore, in this paper, the graphs of the pressure distribution are indicated for the changes in parameters *K*, *E*, *P*, and *h*.

For the traditional FPS design (Fig. 9, a), the change in the load factor K has little effect on the distribution of hydrostatic pressure (Ph), so it changes according to a linear law, but at the same time, the distribution of contact pressure (Pc) changes. At the load factor K = 0.85, a section with a width of 2.5 mm is observed, on which there is no contact pressure. Accordingly, there is no contact between the friction pairs in this section. That is, in this case, 77.5% of the surface of the friction pair is in contact. As the value of the coefficient K increases, this section decreases, and at a value of *K* = 1.1, full contact is observed along the friction pair width. A sharp jump in contact pressure values is observed in the area of contact from 8.5 to 9 mm, which is caused by a decrease in the hydrostatic pressure indicator to zero. The maximum values of the contact pressure are not displayed on the graph and are presented separately in Table 6. The results obtained for the traditional FPS design are taken as a baseline, and further comparisons are made with respect to them.

For the FPS design with an annular plate, the effect of changing the factor K is the same as for the traditional FPS design (Fig. 9, b). The main difference is that there is a decrease in the contact pressure indicators in the areas close to the exit from the seal. And as a result, there is a decrease in the maximum contact pressure indicators (Table 6). On average, the value of the contact pressure decreased by 3%.

In the case of the FPS model with grooves in the annular plate (Fig. 9, c, d), a change in the distribution of hydrostatic pressure along the width of the friction pair is observed at the load factor *K* = 0.9. When considering the line running along the groove (Fig. 9, c), the contact area is the smallest and is 1.5 mm, which means that only 13.5 % of the friction pair surface is in contact. Along the line passing through the place of the plate (Fig. 9, d), the contact width reaches 5 mm. That is, 45 % of the surface of the friction pair is in contact in this place.

It is worth noting that for all cases, the contact pressure value at the groove level decreases, but at the plate level, it increases and becomes higher than the indicators of the FPS model with an annular plate.

The sealing at *K* = 0.85 becomes impossible since the critical value of the pressure force transmitted from the CFX solver to the solid model solver is reached. At the same time, the contact between the bushing support disk and the packing is completely broken, which makes it impossible to solve the problem further. In practice, this means that the hydrostatic pressure squeezes the packing so much that it ceases to perform the role of a sealant and this causes a high level of leakage through the seal.

When the coefficient K increases (*K* = 0.95, 1.0, and 1.1), the graph of the hydrostatic pressure distribution becomes less complete, but the pressure drop remains different from the linear law. The distribution of contact pressure becomes more like the basic version of the design, but at the same time, most of its values are smaller on average by 27 %. A sharp jump in contact pressure values is observed only in the area from 8 to 9 mm. Therefore, the maximum values of the contact pressure are higher than the indicators of the basic design by 85 % along the line with a groove and by 110 % along the line of a plate (Table 6).

Here figures c and d show the hydrostatic and contact pressure distribution on the groove and plate lines shown in Fig. 3

Table 6 – The value of the maximum contact pressure for the FPS design when the load factor K changes

No.	The value of the load factor *K*	The value of the maximum contact pressure Pc_{max} (MPa) for FPS designs			
		Traditional	With an annular plate at the bottom of the stuffing box	With grooves in the annular plate	
				On groove line	On plate line
1	0.85	0.438	0.424	–	–
2	0.90	0.423	0.454	0.701	0.934
3	0.95	0.495	0.481	0.924	1.000
4	1.00	0.529	0.512	0.973	1.021
5	1.10	0.577	0.560	1.152	1.278

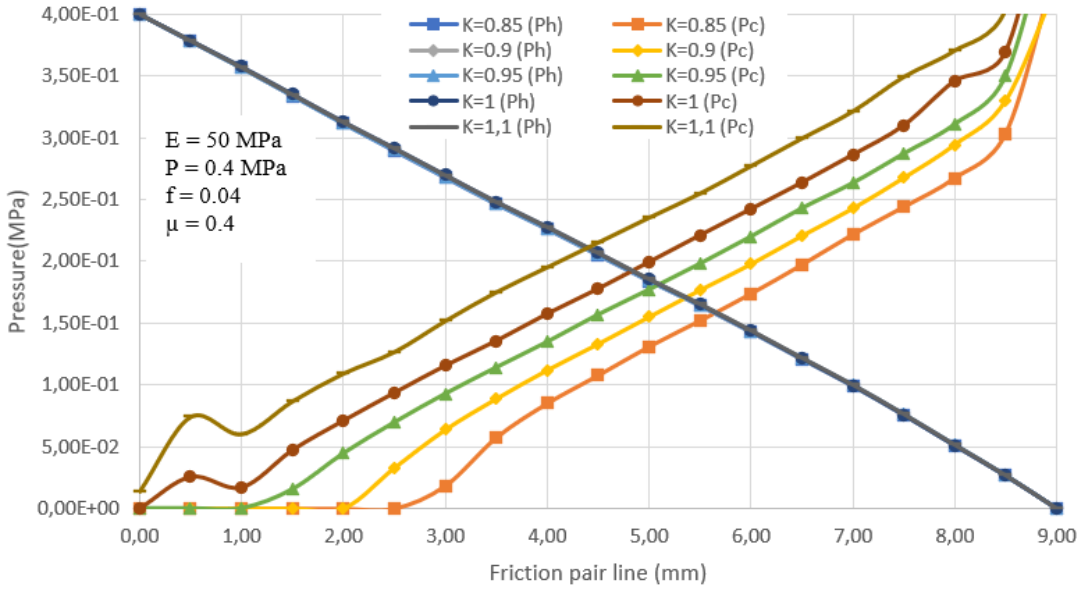

a

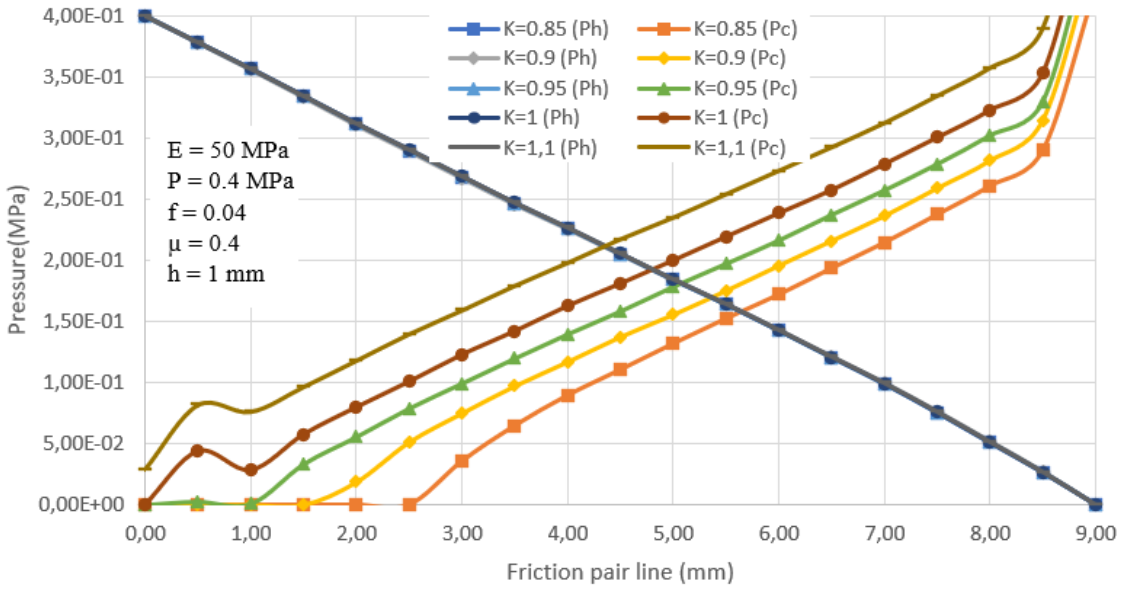

b

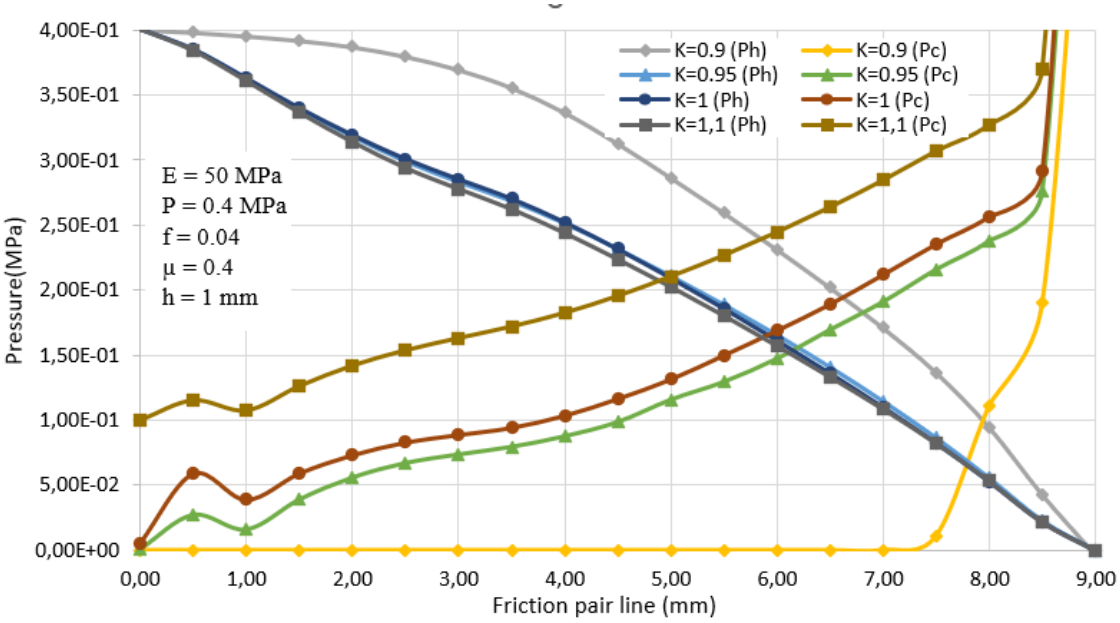

c

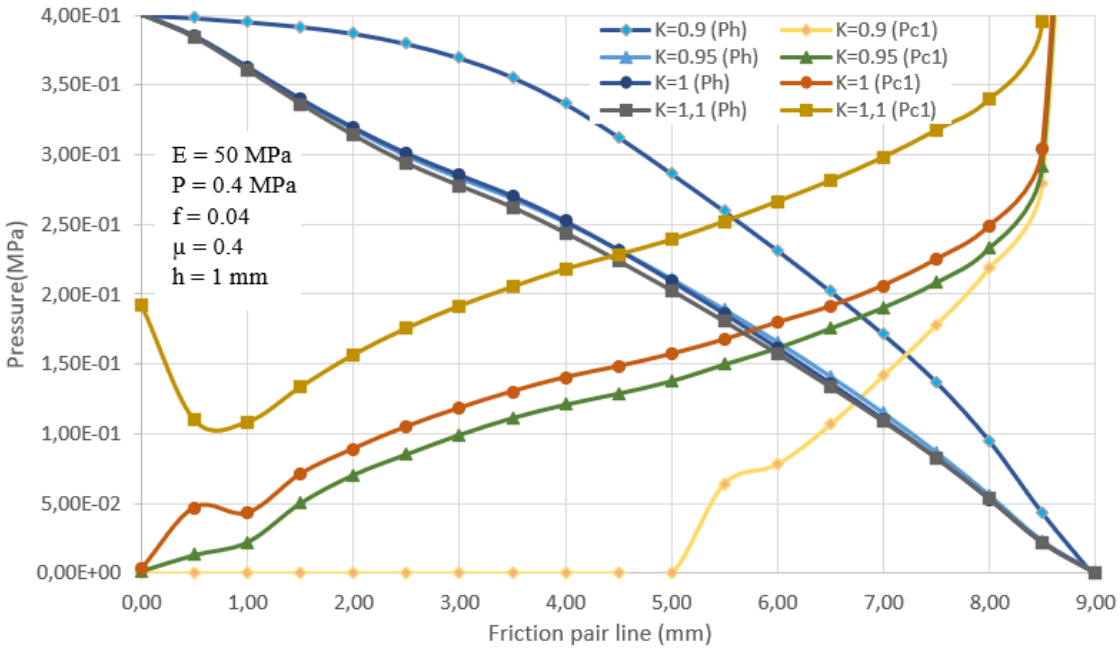

d

Figure 9 – Hydrostatic P_h and contact P_c pressure distribution, which depends on load coefficient K for classic face seal (a), face seal with bottom plate (b), and face seal with grooves in the bottom plate (c, d)

4.2 Parameter *E* influence analysis

For the traditional FPS design (fig. 10, a), the change in Young's modulus does not significantly affect the hydrostatic or contact pressure change. Their distribution remains almost linear. Contact is observed over the entire width of the friction pair.

A change in the shape of the contact pressure distribution with an increase in Young`s modulus value is observed for the FPS design (fig. 10, b) with an annular plate.

In this case, the stiffness of the structural pair of packing + annular plate changes in such a way that the contact pressure tries to equalize. That is, in the area towards the center of the friction pair width (from 0 to 4.75 mm), the contact pressure increases, while in the area after the center (from 4.75 to 9.0 mm), the contact pressure decreases. It will be useful to use this property when designing the FPS design with the best parameter combination.

For the design of the FPS with grooves in the plate (Figures 10c-d), a change in hydrostatic pressure distribution is observed when Young's modulus increases.

The graph of hydrostatic pressure distribution becomes fuller. At the same time, the distribution of contact pressure decreases with an increase in Young's modulus value, but in general, it repeats the picture shown in Fig. 9c-d for the load factor $K = 1$.

Table 7 shows the indicators of the maximum hydrostatic and contact pressures, which are unmarked on the graphs (Fig. 10).

Figures 10c-d show the hydrostatic and contact pressure distribution on the groove line and plate line, shown in Fig. 3.

Table 7 – The value of the maximum contact pressure for the design of the FPS when Young's modulus E changes

No.	Young's modulus (MPa)	The maximum contact pressure P_{Cmax} (MPa) for FPS designs			
		Traditional	With an annular plate	With grooves in the annular plate	
				On groove line	On plate line
1	50	0.529	0.512	0.972	1.021
2	150	0.529	0.485	0.804	0.917
3	250	0.527	0.462	0.802	0.881
4	350	0.526	0.444	0.761	0.852

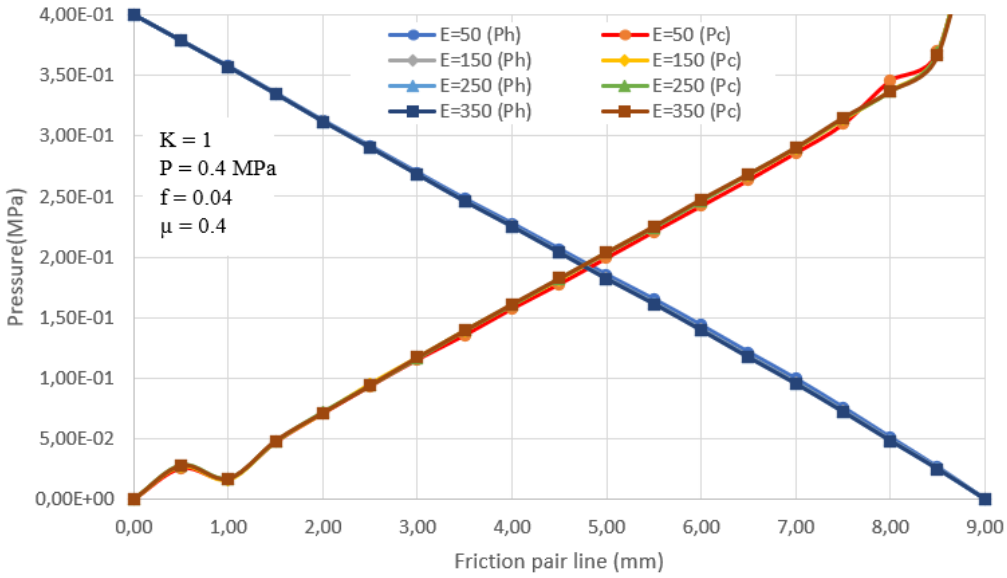

a

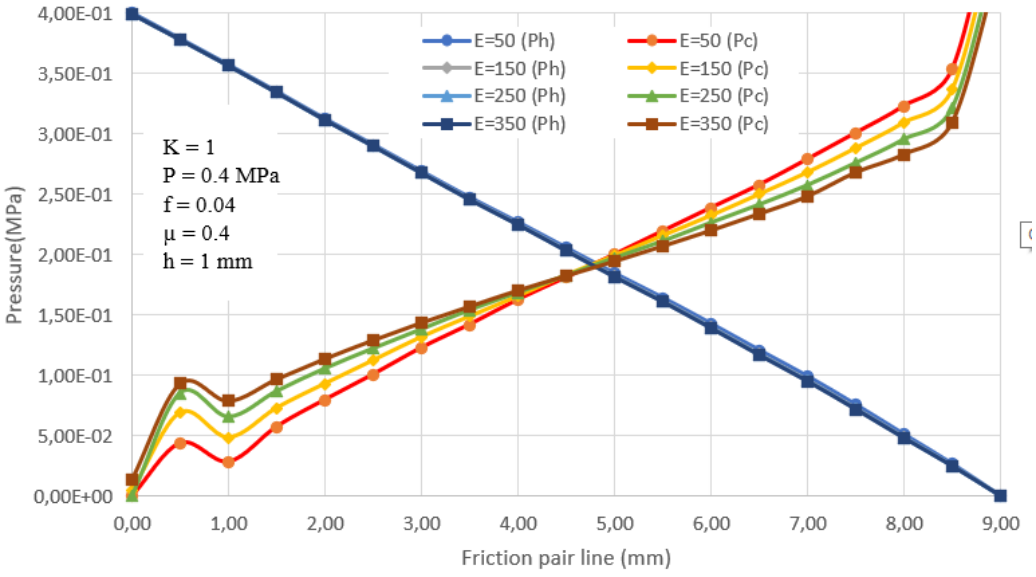

b

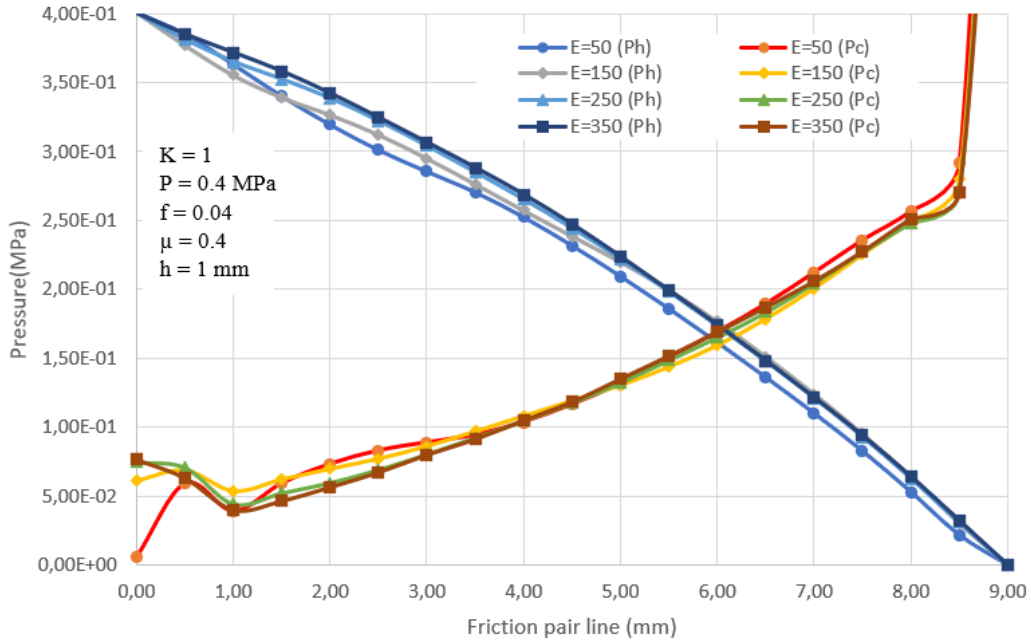

c

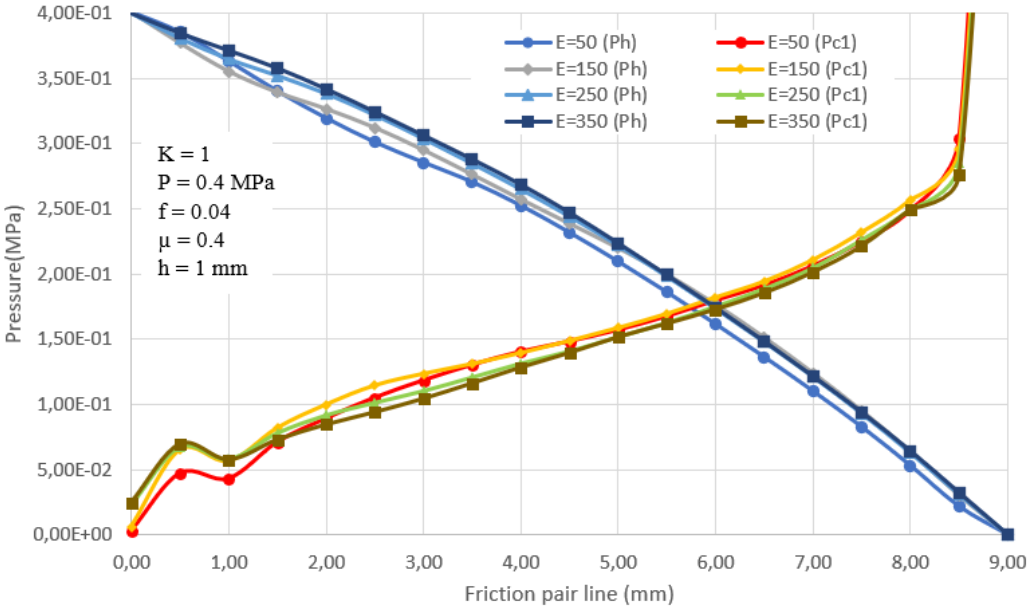

d

Figure 10 – Hydrostatic P_h and contact P_c pressure distribution, which depends on Young's modulus E for classic face seal (a), face seal with bottom plate (b), and face seal with grooves in the bottom plate (c, d)

4.3 Parameter *P* influence analysis

All three designs do not have significant differences depending on the input pressure value (Fig. 11). Pressure distributions change proportionally with increasing inlet pressure. Also, regardless of the value of the input pressure, a contact is present over the entire width of the packing, provided by the load factor K=1.

Separately, Table 8 lists the values of the maximum contact pressure, which are not shown on the graphs (Fig. 11).

Figures 11c-d show the hydrostatic and contact pressure distribution on the groove line and plate shown in Fig. 3.

Table 8 – Values of the maximum contact pressure for the FPS design when the inlet pressure *P* changes

No.	Inlet pressure, MPa	The value of the maximum contact pressure Pc_{max} (MPa) for FPS structures			
		Traditional	With an annular plate	With grooves in the annular plate	
				On groove line	On plate line
1	0.4	0.529	0.512	0.972	1.021
2	0.8	1.047	1.022	1.916	2.147
3	1.2	1.573	1.522	2.497	3.227
4	1.6	2.037	2.000	3.474	4.513

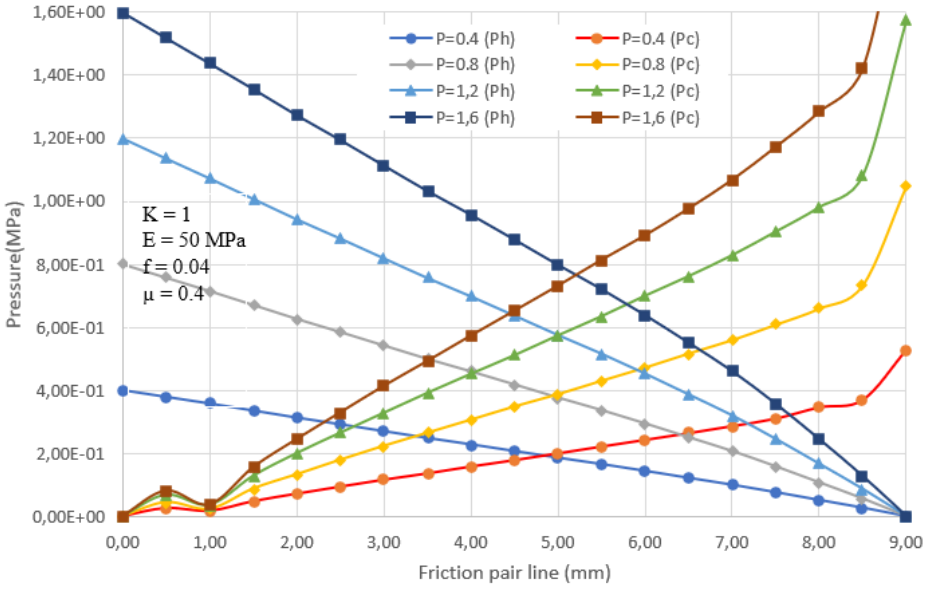

a

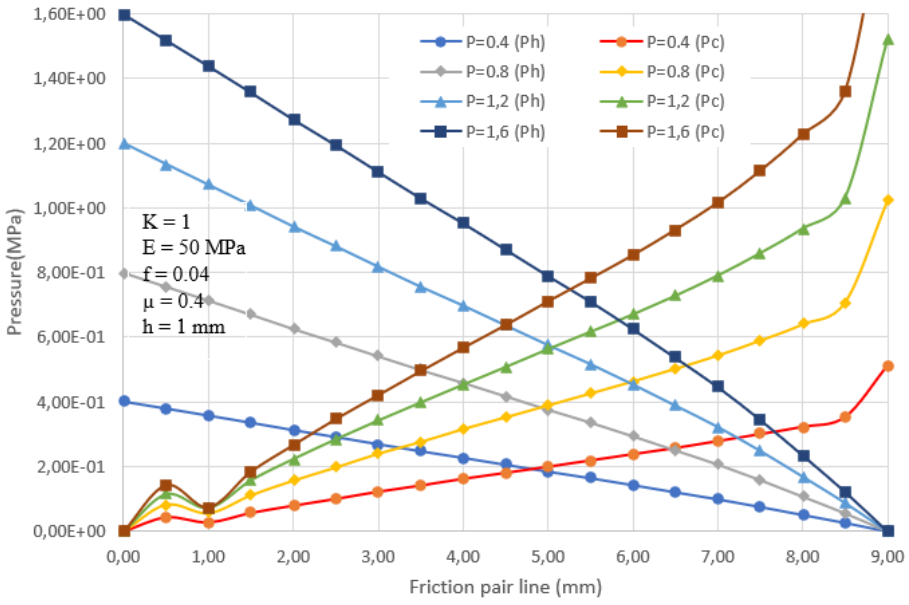

b

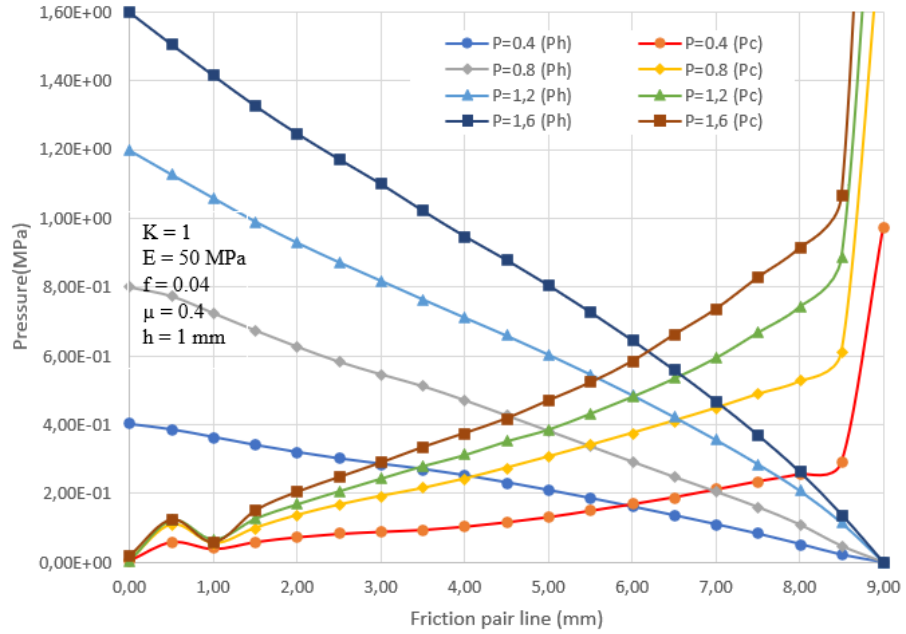

c

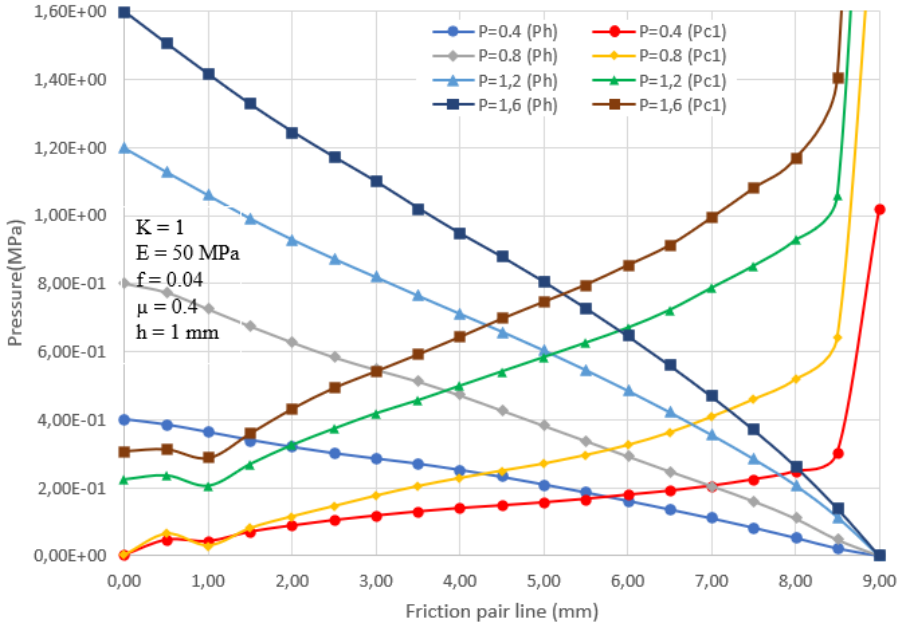

d

Figure 11 – Hydrostatic P_h and contact P_c pressure distribution which depends on inlet pressure P for classic face seal (a), face seal with bottom plate (b), and face seal with grooves in the bottom plate (c, d)

4.4 Parameter *h* influence analysis

A decrease in the thickness of the plate influences the distribution of contact pressure (Fig. 12). A tendency to equalize the contact pressure is observed, similar to the situation with Young's modulus change. But unlike Young's modulus, the limit of reducing the plate thickness is determined by the strength and rigidity of the FPS design. Thus, using a plate with a thickness of less than 0.3 mm leads to a loss of rigidity and eliminates any sense of its use at the bottom of the stuffing box.

It can also be noted that, for a design with a plate, there is no effect on hydrostatic pressure distribution by a change in the plate thickness (Fig. 12a). For the FPS design with a groove in the plate, as the plate thickness decreases, the hydrostatic pressure curve gradually approaches a linear law, i.e., its filling decreases. When the thickness of the plate is less than 0.5 mm, the opposite situation is observed - the distribution becomes less filled and more concave. Thus, a slight increase in contact pressure is observed, and the most significant degree of its alignment is ensured.

Table 9 – The value of the maximum contact pressure for the FPS design when the plate thickness changes *h*

No.	Plate thickness, mm	The value of the maximum contact pressure Pc_{max} (MPa) for FPS designs		
		With an annular plate	With grooves in the annular plate	
			On groove line	On plate line
1	0.3	0.376	0.626	0.852
2	0.5	0.445	0.818	0.989
3	0.8	0.499	0.917	1.007
4	1.0	0.512	0.972	1.021

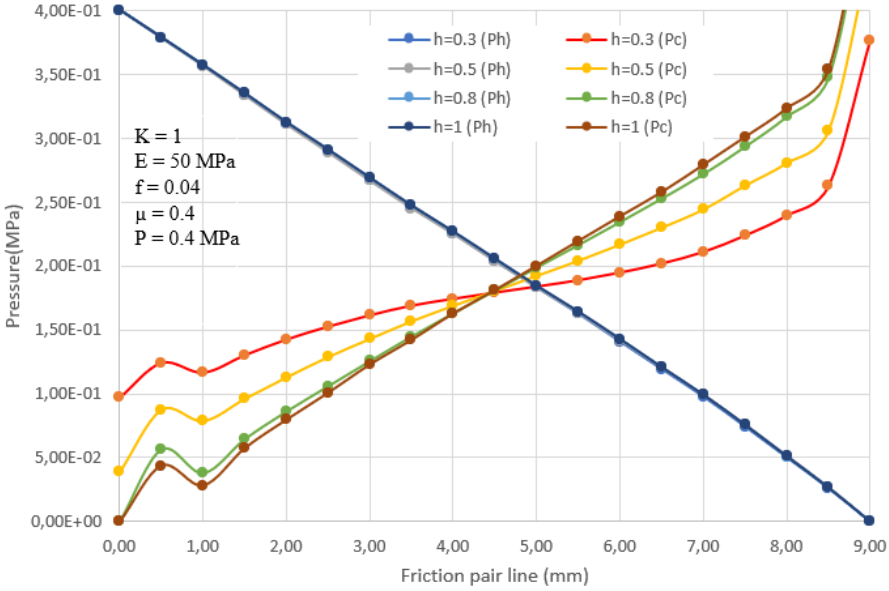

a

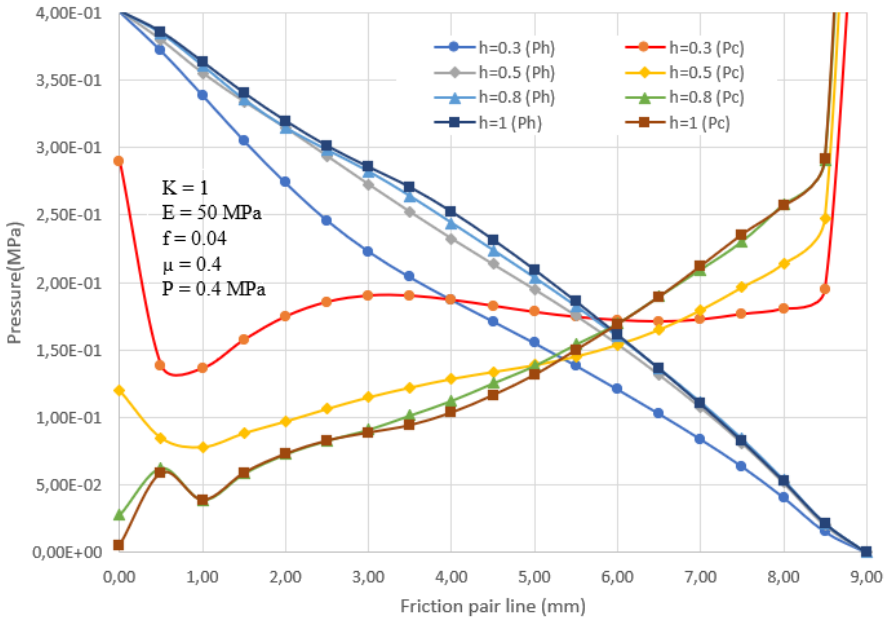

b

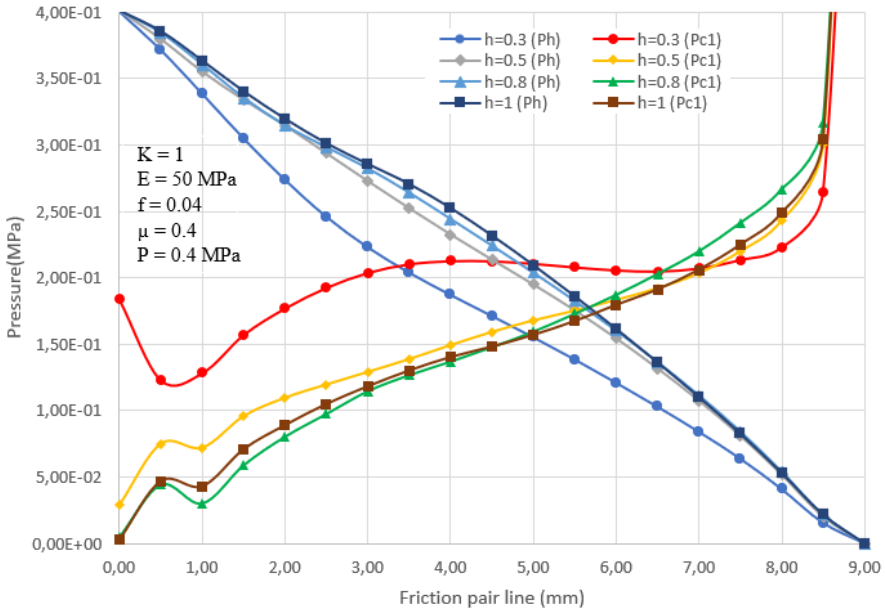

c

Figure 12 – Hydrostatic P_h and contact P_c pressure distribution which depends on plate thickness h for face seal with bottom plate (a) and face seal with grooves in the bottom plate (b, c)

4.5 Analysis of research. Choosing the FSP design with the best parameters combination

Based on the computer simulation results, the following points can be identified that are useful for practical use. Firstly, the design of the FPS with grooves in the annular plate at the bottom of the stuffing box allows you to generally reduce the amount of contact pressure across the width of the friction pair. Secondly, changing parameters E and h create conditions for equalizing the contact pressure on the same contact area. Thus, based on the results described above, it is possible to propose an FPS design with the best parameter combination.

Comparative Table 10 presents combinations of FPS designs and parameters that indicate the impracticality of the combination (red), the possibility of combination, but not a high degree of improvement in indicators (yellow), lack of influence (gray) and the best designs (green).

Thus, the best FPS design is a design with an annular plate and with grooves in the annular plate at E = 350 MPa and h = 0.3 mm. The simulation was carried out with the following parameters (Table 11). Fig. 13 shows that the combination of parameters E and h ensures equalization of the contact pressure across the friction pair width than the parameters taken separately.

Figures 13, 14 show the distribution of hydrostatic and contact pressures along the friction pair width for FPS designs with the best parameter combination.

After analyzing the given graphs, the following conclusions can be reached. In the design of the FPS with an annular plate, smooth equalization of the contact pressure is performed (without sharp peak values of the contact pressure), which subsequently has a positive effect on the intensity of wear of the entire surface of the packing in the place of contact with the support disk.

At the same time, an insignificant leakage rate is achieved. At the same time, in the FPS design with grooves in the annular plate, the peak value of the contact pressure is preserved closer to the exit from the seal. However, the overall value of the contact pressure distribution is smaller than in the FPS design with an annular plate. At the same time, the leakage rate is also smaller (Table 12).

Table 10 – A comparative analysis

No.	Parameter	The value of the parameter	FPS design		
			Traditional	With annular plate at the bottom of the stuffing box	With a groove in the annular plate
1	Load factor *K*	0.85		–	–
		0.90			
		0.95			
		1.00			
		1.10			
2	Young's modulus *E*, MPa	50			
		150			
		250			
		350			
3	Inlet pressure *P*, MPa	0.4			
		0.8			
		1.2			
		1.6			
4	Plate thickness *h*, mm	0.3	–		
		0.5	–		
		0.8	–		
		1.0	–		

Table 11 – Modeling the FPS designs with the best parameters combination

	Parameter	Marking	Size
1	Inlet pressure	*P*	0.4 MPa
2	Shaft rotation frequency	*n*	3000 rpm
3	The annular plate thickness	*h*	0.3 mm
4	The height of the average gap	h_{gap}	3 μm
5	Load factor of the support disk	*K*	1
6	Young's modulus	*E*	350 MPa
7	Poisson's ratio	*μ*	0.4
8	Friction coefficient	*f*	0.04

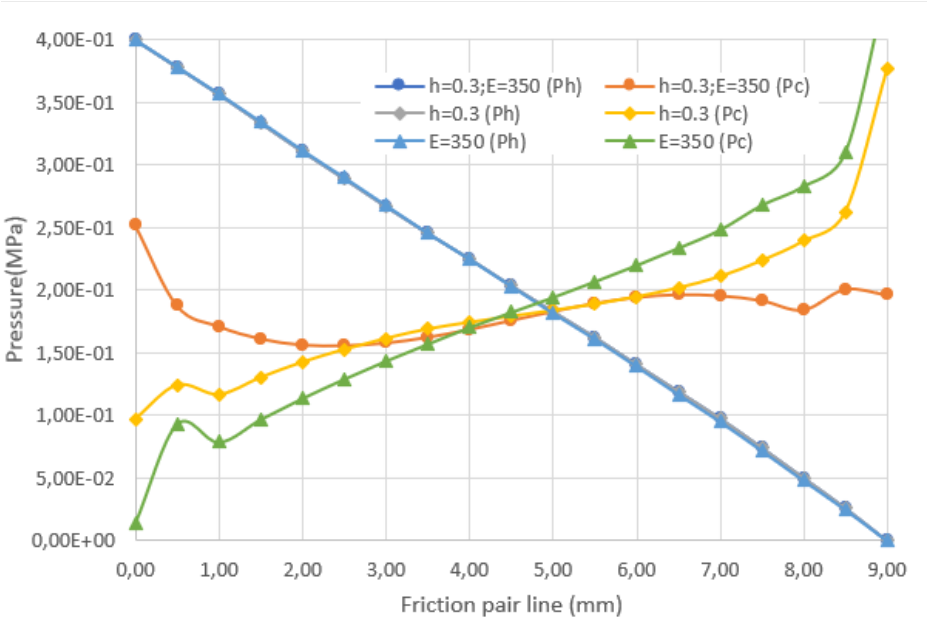

Figure 13 – Hydrostatic P_h and contact P_c pressure distribution for face seal with the annular plate

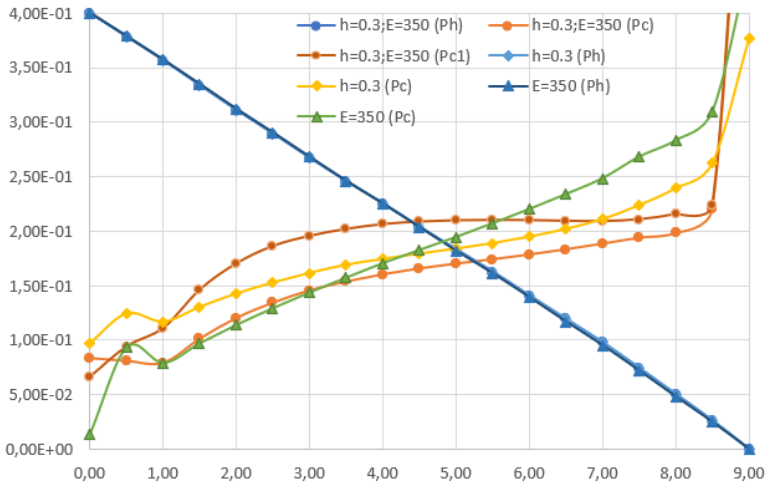

Figure 14 – Hydrostatic P_h and contact P_c pressure distribution for face seal with grooves on the plate

4.6 Leakage rate analysis

In addition to the hydrostatic and contact pressure distributions, the leakage rate is an essential parameter of the seal operation. Table 12 lists the values of leakage for all the above-mentioned FPS designs.

When summarizing the obtained results, it can be noted that the leakage rate decreases when the coefficients *K*, *E*, and *h* increase. In principle, the leakage size differs only in the case of a change in the inlet pressure. For all FPS designs, the maximum amount of leakage is achieved at an inlet pressure of 1.6 MPa.

Separately, it can be noted that for the FPS design with a groove in the annular plate where at the load factor $K = 0.9$ there is a sharp increase in the leakage rate (almost 3 times) compared to other values of the K factors. A similar picture is observed for the parameter $h = 0.3$ mm.

However, in this case, the leakage rate increases by only 18 %.

Comparing different FPS designs, it can be noted that the leakage rate for the annular plate FPS design is, on average 5 % lower compared to the traditional FPS design. And the leakage rate for the FPS design with a groove in the annular plate is, on average, 4.5 % higher than the leakage of the traditional FPS design.

The leakage rate of FPS in terms of contact pressure distribution is 0.0607 l/h for the FPS design with an annular plate, which is 0.2 % lower than the indicators of the traditional FPS design and 0.0614 l/h for the FPS design with a groove in the annular plate - which is higher by 0.9 % for indicators of the conventional FPS design.

Thus, the FPS design quality depends to a greater extent on the contact pressure distribution since the change in the leakage rate for different FPS designs is insignificant.

Table 12 – The leakage rate with different parameters and FPS designs

No.	Parameter	Value	The number of leakage for FPS designs, 1/h		
			Traditional	With an annular plate	With a groove
1	Load factor *K*	0.85	0.06172	–	–
		0.90	0.06174	0.06270	0.18548
		0.95	0.06160	0.06128	0.06452
		1.00	0.06124	0.06123	0.06417
		1.10	0.06137	0.06127	0.06322
2	Young's modulus *E*, MPa	50	0.06124	0.06123	0.06417
		150	0.06088	0.06085	0.06261
		250	0.06081	0.06077	0.06221
		350	0.06079	0.06074	0.06233
3	Inlet pressure *P*, MPa	0.4	0.06124	0.06123	0.06417
		0.8	0.12473	0.12401	0.12255
		1.2	0.18943	0.18770	0.19139
		1.6	0.25856	0.25234	0.25387
4	Plate thickness *h*, mm	0.3	–	0.06139	0.08336
		0.5	–	0.06199	0.06762
		0.8	–	0.06121	0.06440
		1.0	–	0.06123	0.06417
Optimal FPS designs		With annular plate		With a groove in the annular plate	
		0.06066		0.06139	

5 Conclusions

The developed computer model allows for solving a complex problem that combines the solution of the hydroelasticity problem and the contact problem. This is the first successful attempt to develop a model with two-way coupling for FPS. The obtained results have differences from the results obtained experimentally. In the experiment, the graph of the hydrostatic pressure distribution is more filled and is described by the Poiseuille equation. The pressure distribution in the presented computer model is reduced to Darcy's equation. Except for the case of the FPS design with a groove in the annular plate at the load factor K = 0.9. This means that some parameters must be considered when building a model. Finding these parameters is the next goal for improving the model.

When comparing different FPS designs, it is observed that the presence of an annular plate leads to a decrease in contact pressure along the friction pair width. At the same time, the leakage rate increases, which is confirmed experimentally.

Nevertheless, the created model made it possible to determine the parameters that most affect the distribution of contact pressure over the width of the friction pair. This, in turn, made it possible to determine the FPS design with the best parameter combination in which equalization of the contact pressure is achieved. In practice, this means that the stuffing box in this operation mode will have more uniform wear, and therefore the seal's service life will be increased.

6 Acknowledgments

Sumy State University supported this research within the project "Analysis of the Influence of Hydrodynamic Forces Acting in Narrow Clearances of Seals and Bearings on Increasing Energy Efficiency and Reducing the Harmful Emissions and Vibrations of Centrifugal Machines" (No. 0120U102004) funded by the Ministry of Education and Science of Ukraine.

References

1. Kovanova, O. (2018). Climate change modeling in the context of urban decarbonization strategy. *Journal of Engineering Sciences*, Vol. 5(1), pp. H1-H6, https://doi.org/10.21272/jes.2018.5(1).h1
2. Hurets, L.L., Kozii, I.S., Miakaieva, H.M. (2017). Directions of the environmental protection processes optimization at heat power engineering enterprises. *Journal of Engineering Sciences*, Vol. 4(2), pp. G12-G16, https://doi.org/10.21272/jes.2017.4(2).g12
3. Martsynkovskyy, V.A. (2005). Hermomechanics, its role in ensuring the efficiency and environmental friendliness of pumping and compressor equipment. *Bulletin of Sumy State University, Series "Technical Sciences"*, Vol. 1(73), pp. 5-10.
4. Marcinkovsky, V.A., Zagorulko, A.V. (1998). Studies of sealed end seals. *Proceedings of International Science and Technology. Conference "Progressive Engine and Technology of Machine Building, Instrument Building and Welding Production"*, Vol. 3, pp. 322-327.
5. Löhner, R., Cebral, J.R., Yang, C., Baum, J.D., Mestreau, E.L., Soto, O. (2006). Extending the range and applicability of the loose coupling approach for FSI simulations. *Fluid-Structure Interaction*, Vol. 53, pp. 82-100, https://doi.org/10.1007/3-540-34596-5_4
6. Zahorulko, A.V. (1999). Research of the processes of friction and sealing in the front oil seal. *Mashinoznavstvo*, Vol. 8(26), pp. 45-48.
7. Gaft, J., Zahorulko, A., Martsynkovskyy, V., Shevchenko, S. (2000). Face packing seals: new opportunities for pump rotor hermetic sealing. *Proceedings of the XVI International Conference "Fluid Sealing. Successful Sealing", Brugge, Belgium*, pp. 335-349.
8. Zahorulko, A., Gudkov, S. (2010). Solution of problem concerning elastohydrodynamic lubrication for friction pair of face packing seal. *Proceedings of the XIII International Conference on Sealing Technology, Stuttgart, Germany*, pp. 317-326.
9. Bouzid, A.H. (2021). A study on liquid leak rates in packing seals. *Applied Sciences*, Vol. 11(4), 1936, https://doi.org/10.3390/app11041936
10. Macdonald, I., El-Sayed, M., Mow, K., Dullien, F. (1979). Flow through porous media – The Ergun equation revisited. *Ind. Eng. Chem. Fundam.*, Vol. 18, pp. 199-208.
11. Diany, M., Bouzid, A.H. (2009). Analytical evaluation of stresses and displacements of stuffing-box packing based on a flexibility analysis. *Tribology International*, Vol. 42(6), pp. 980-986, https://doi.org/10.1016/j.triboint.2009.02.002
12. Diany, M., Bouzid, A.H. (2009). Short term relaxation modeling of valve stem packings. *Journal of Tribology*, Vol. 131(3), 032201, https://doi.org/10.1115/1.3118787
13. Greenwood, J.A., Williamson, J.B.P. (1966). Contact of nominally flat surfaces. *Proceedings of the Royal Society of London. Series A, Mathematical and Physical Sciences*, Vol. 295(1442), pp. 300-319.
14. Zahorulko, A.V. (2001). *Research on the Mechanism of Sealing and Development of Methods of Calculation and Design of End Packings of Sealed Rotors of Pumps*. Ph.D. Thesis, Sumy State University, Sumy, Ukraine.
15. Cook, R., Malkus, D., Plesha, M., Witt, R. (2002). *Concepts and Applications of Finite Element Analysis*. John Wiley & Sons, Inc.